

The defective nature of CdSe quantum dots embedded in inorganic matrices

Wenke Li,^{1,2} Kai Li,¹ Xiujian Zhao,¹ Chao Liu,^{1,*} François-Xavier Coudert^{2,*}

¹ State Key Laboratory of Silicate Materials for Architectures, Wuhan University of Technology, Hubei, 430070, China

² Chimie ParisTech, PSL University, CNRS, Institut de Recherche de Chimie Paris, 75005 Paris, France

E-mail: hite@whut.edu.cn

fx.coudert@chimieparistech.psl.eu

Table S1 The simulated compositions and sizes of each glasses.

| Model | Cell Size (Å) | Number of Atoms | | | | | |
|------------|------------------|-----------------|-----|-----|----|----|----|
| | | O | Si | Na | Ca | Cd | Se |
| Q25N75S | 19.383 | 210 | 90 | 60 | -- | 33 | 33 |
| Q33N67S | 19.383 | 195 | 78 | 78 | -- | 33 | 33 |
| Q20N5C75S | 25.34 | 595 | 255 | 136 | 17 | 33 | 33 |
| Q15N10C75S | 25.227 | 595 | 255 | 102 | 34 | 33 | 33 |

Table S2 Excitation of Cd₃₃Se₃₃ quantum dots embedded in different glass matrix. In the table, excitation energies (E_{exc}), oscillator strength (f), and percentage of contribution of transitions from each orbital to LUMO of the lowest-energy transition as well as the strongest transition are reported. All contributions higher than 5% are listed.

| Model | E_{exc} | f | Percentage | Excited-States Composition |
|------------|-----------|--------|--------------|----------------------------|
| Q25N75S | 2.25 | 0.30 | 97.74% | HOMO→LUMO |
| Q33N67S | 2.23 | 0.016 | 98.06% | HOMO→LUMO |
| | 2.58 | 0.195 | 89.22% | HOMO-5→LUMO |
| Q20N5C75S | 2.22 | 0.113 | 93.63% | HOMO→LUMO |
| | 2.57 | 0.145 | 89.29% | HOMO-3→LUMO |
| Q15N10C75S | | | 76.91% | HOMO→LUMO |
| | 2.35 | 0.051 | 10.78% | HOMO-2→LUMO |
| | | | 7.86% | HOMO-1→LUMO |
| | 2.94 | 0.161 | 42.65% | HOMO-13→LUMO |
| | | 28.13% | HOMO-14→LUMO | |

Table S3 Dielectric constant of glass matrix. The dielectric constant of glass can be calculated by adding the dielectric constant of each glass component. x_i represents the molar percentage of the i^{th} component with a dielectric constant of ϵ_i .

| Component | Dielectric Constant | Model | Dielectric Constant |
|--|---------------------|------------|---------------------|
| Na ₂ O | 17.6 | Q25N75S | 7.25 |
| CaO | 17.4 | Q33N67S | 8.354 |
| SiO ₂ | 3.8 | Q20N5C75S | 7.24 |
| Equation: $\epsilon = \sum_i x_i \epsilon_i$ | | Q15N10C75S | 7.23 |

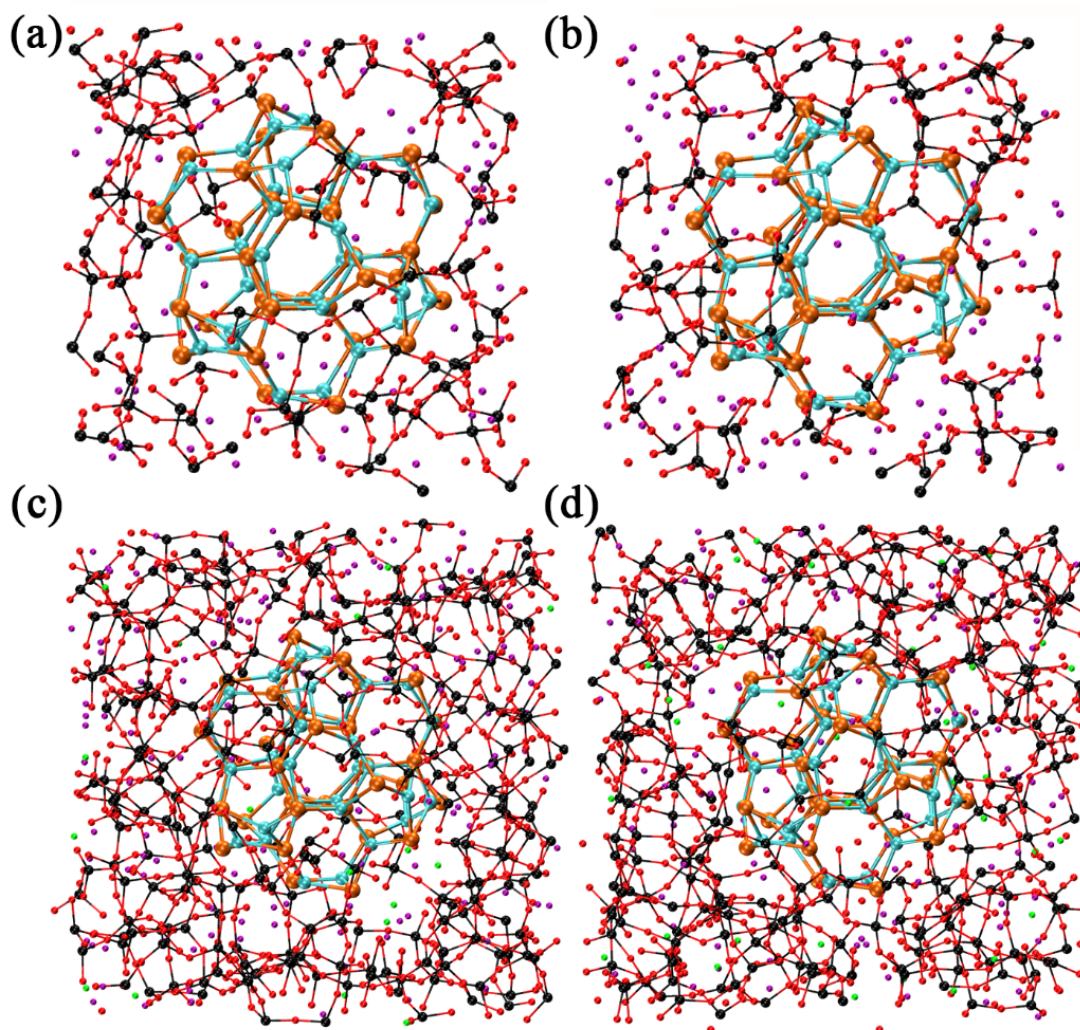
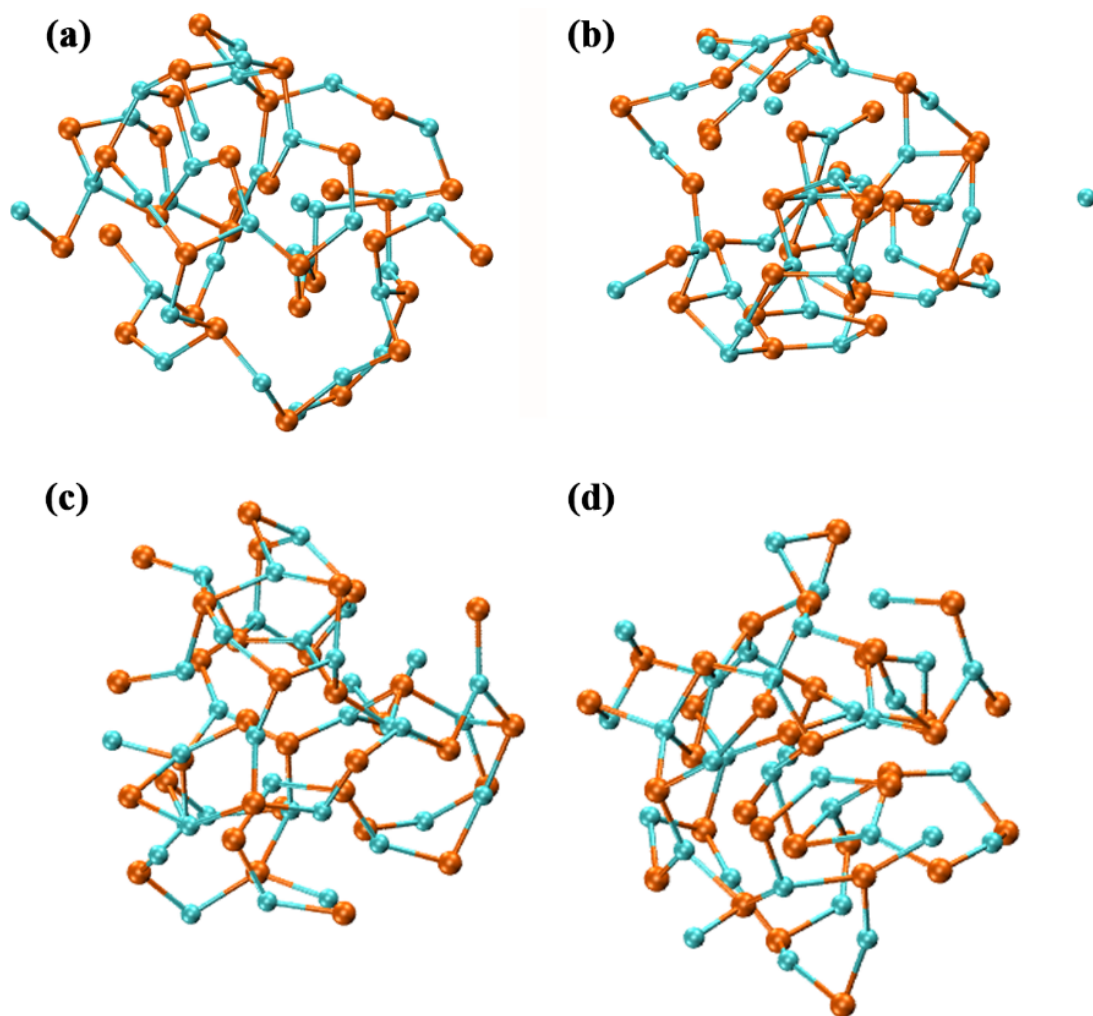
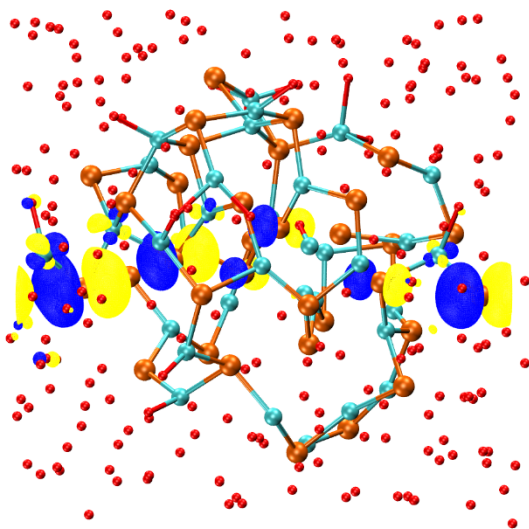


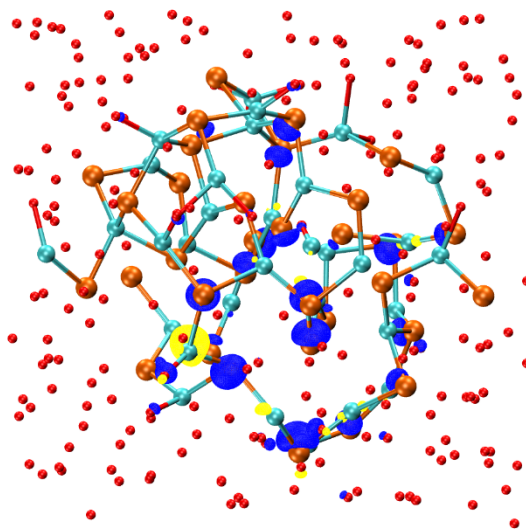
Figure S1 Initial configuration of the classical molecular dynamics to generate the atomic structure of CdSe QDs embedded inorganic matrices. Glass composition: (a) 25 Na₂O–75 SiO₂–33 CdSe, (b) 33 Na₂O–67 SiO₂–33 CdSe, (c) 20 Na₂O–5 CaO–75 SiO₂–33 CdSe, and (d) 15 Na₂O–10 CaO–75 SiO₂–33 CdSe. The color of the atoms are: Cd in cyan, Se in orange, O in red, Si in black, Na in purple, Ca in green.



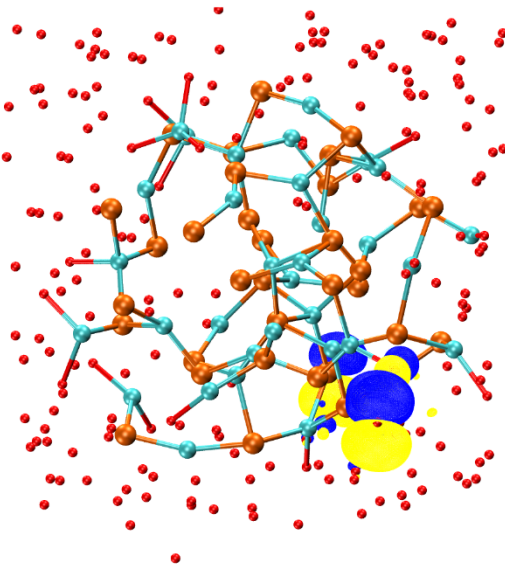
(a) Q25N75S HOMO



(b) Q25N75S LUMO



(c) Q33N67S HOMO



(d) Q33N67S LUMO

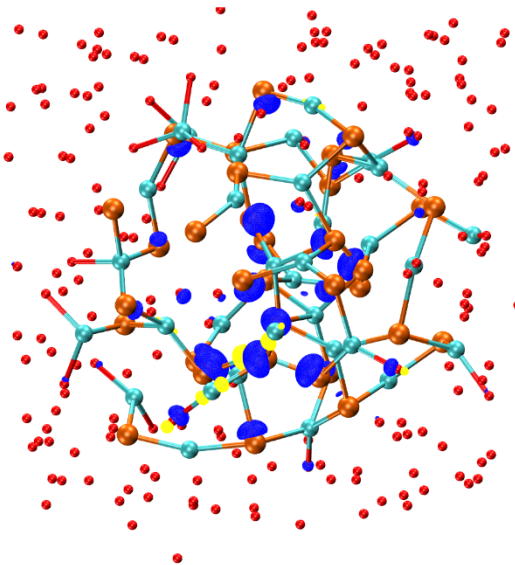


Figure S3 Plots of the HOMO and LUMO of Q25N75S and Q33N67 glasses. To give a clear illustration about the electron density distribution of HOMO, only O (near the QD), Cd and Se atoms are selected to be shown.

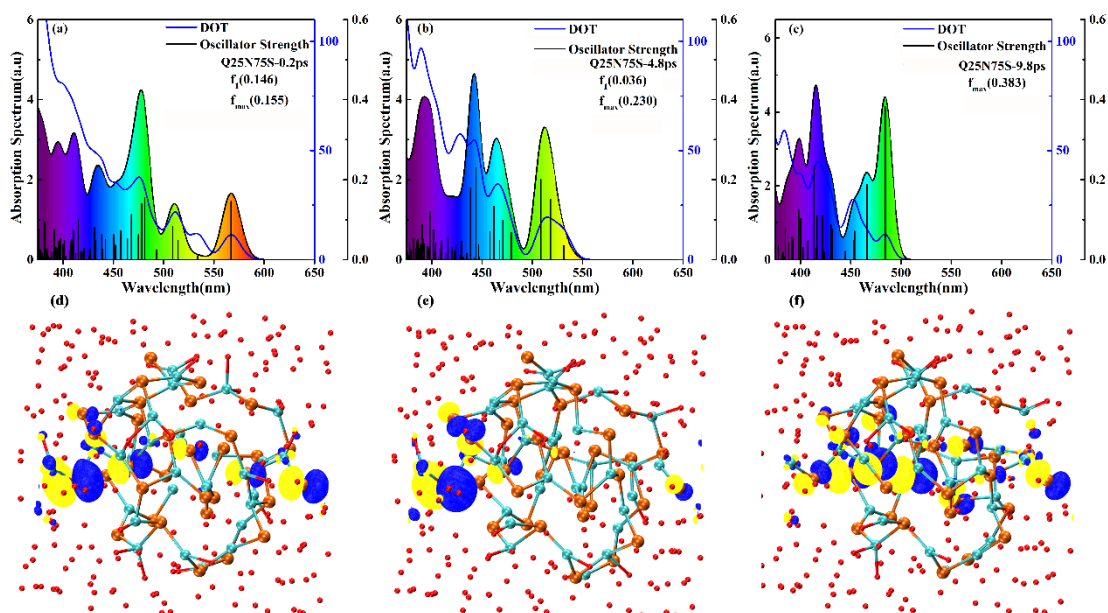


Figure S4 Absorption spectrum of Q25N75S glass and plots of the HOMO. Absorption spectrum (black line, shaded) and density of transitions (blue line). Black vertical bars show individual excited states, with the values for the oscillator strength shown at the right y-axis. The configurations were taken from the 10 ps *ab initio* molecular dynamics run at (a) 0.2 ps, (b) 4.8 ps, (c) 9.8 ps. We have calculated HOMO-LUMO gap of 50 configurations selected from production run and these three configurations are with the smallest HOMO-LUMO gap, HOMO-LUMO gap equal to pristine QD, and largest HOMO-LUMO gap, respectively. To give a clear illustration about the electron density distribution of HOMO, only O (near the QD), Cd and Se atoms are selected to be shown in (d)-(f).

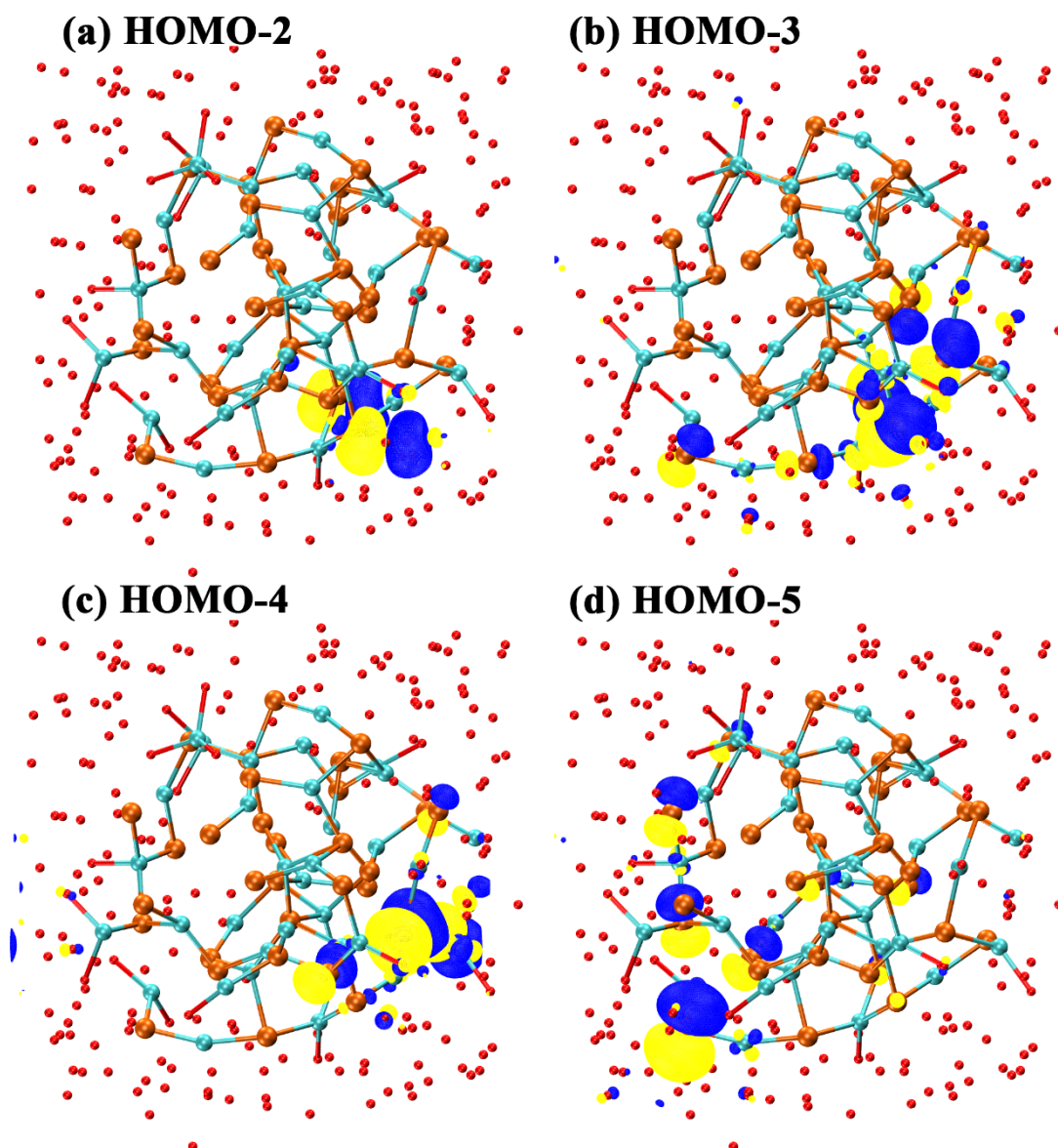


Figure S5 Molecular orbitals of Q33N67S glasses. (a) HOMO-2, (b) HOMO-3, (c) HOMO-4, and (d) HOMO-5. To give a clear illustration about the electron density distribution of HOMO, only O (near the QD), Cd and Se atoms are selected to be shown.

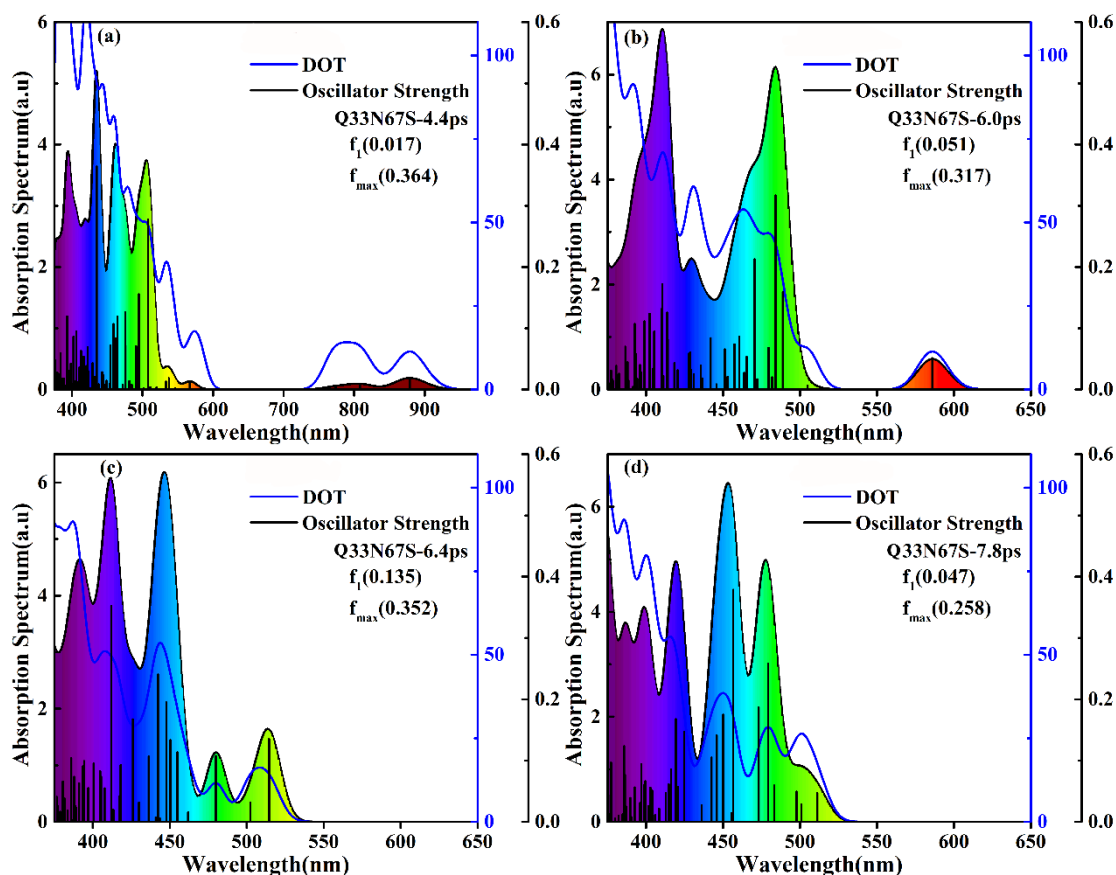


Figure S6 Absorption spectrum of Q33N67S glass. The configuration was selected from the 10 ps production run at (a) 4.4 ps, (b) 6.0 ps, (c) 6.4 ps, and (d) 7.8 ps, respectively. The HOMO was decided by non-bridging oxygen atoms for (a) and (d) while it was determined by Se atoms for (b) and (c) based on the analysis of density of states of our previous work (Ref: J. Phys. Chem. C 2021, 125 (34), 18916-18926). The HOMO-LUMO gap of the configuration at 4.4 ps was smallest and at 6.4 ps was highest.

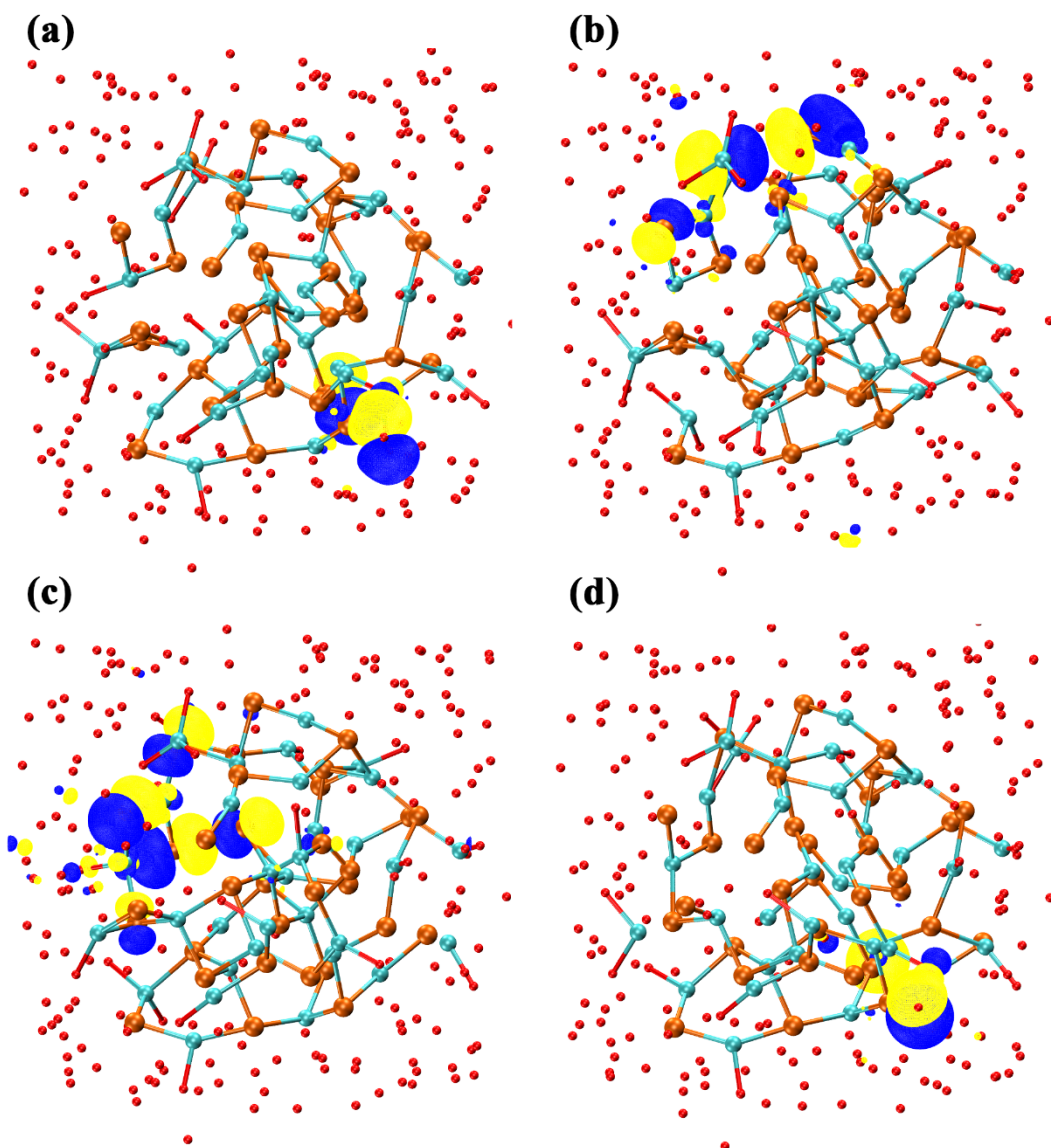


Figure S7 Plots of the HOMO of Q33N67S glasses. Configuration was selected from the 10 ps production run at (a) 4.4 ps, (b) 6.0 ps, (c) 6.4 ps, and (d) 7.8 ps, respectively. To give a clear illustration about the electron density distribution of HOMO, only O (near the QD), Cd and Se atoms are selected to be shown.

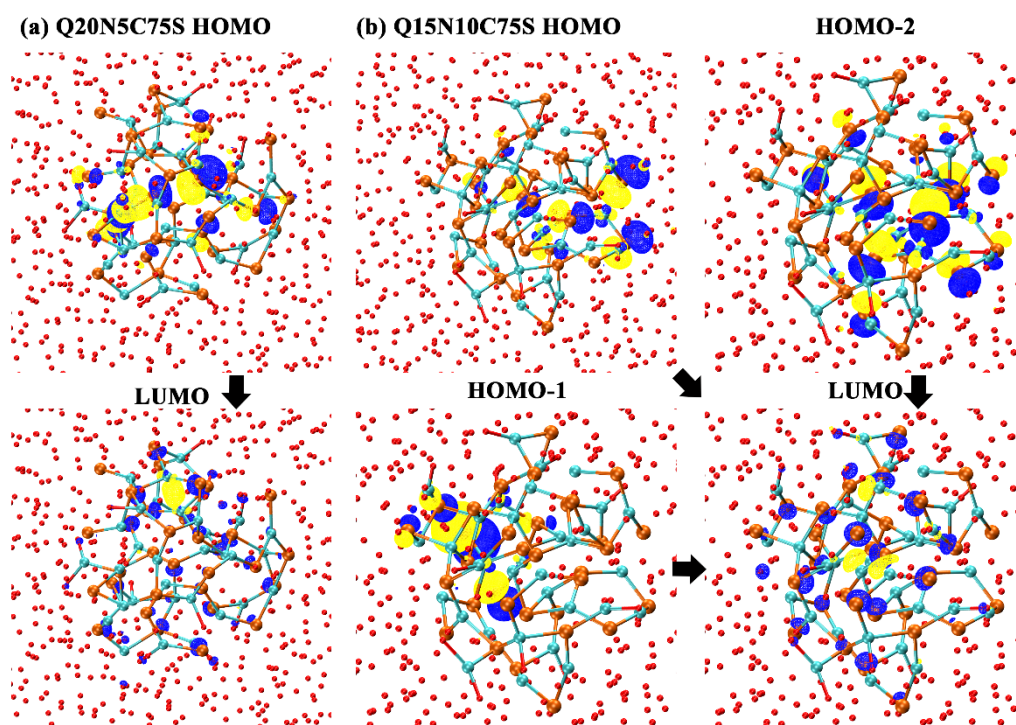


Figure S8 Plots of molecular orbitals of (a) Q20N5C75S glasses and (b) Q15N10C75S glasses. To give a clear illustration about the electron density distribution of HOMO, only O (near the QD), Cd and Se atoms are selected to be shown.

Experimental and Characterization Method

Glasses with nominal compositions (mol%) of 25 Na₂O–75 SiO₂–1 CdSe (Q25N75S), 33 Na₂O–67 SiO₂–1 CdSe (Q33N67S), 20 Na₂O–5 CaO–75 SiO₂–1 CdSe (Q20N5C75S), and 15 Na₂O–10 CaO–75 SiO₂–1CdSe (Q15N10C75S) were fabricated using the conventional melt-quenching method. Raw chemical powders with purity of >99.9% were mixed thoroughly and melted in alumina crucibles at 1400 °C for 40 minutes under the ambient atmosphere. The melts were poured onto a brass mould and quenched by pressing with another plate. The as-obtained glasses were annealed for 3 h to reduce the thermal stress. After annealing, the glasses were cut into small species for further heat-treatment. CdSe QDs were precipitated in the glasses through one-step heat-treatment at 530 °C for 20 h, 480 °C for 20 h, 560 °C for 10 h and 580 °C for 40 h for Q25N75S, Q33N67S, Q20N5C75S and Q15N10C75S glasses, respectively. The absorption spectra of polished specimens were recorded using an UV/vis/NIR spectrophotometer (Lambda 750s, PerkinElmer, USA). The photoluminescence spectra were measured using time-resolved fluorescence spectrometer (FL3-33, Jobin-Yvon, USA) under 365 nm light excitation. The PLQY was recorded by a UV-NIR quantum

yield spectrometer (C13534, Quantaurus-QY Plus, Hamamatsu, Japan), composed of a 3.3-inch integrating sphere, multichannel spectrometer, BT-CCD linear image photo-detector, and 150 W Xenon lamp as excitation light source. The PLQY was calculated based on the ratio between the number of photons emitted by the glass samples and the number of photons absorbed by the specimens ($PLQY = PN_{em}/PN_{ab}$). Laser confocal Raman spectrometer (Invia, Renishaw, UK) equipped with 532 nm laser was applied to record the Raman spectra of heat-treated glasses.

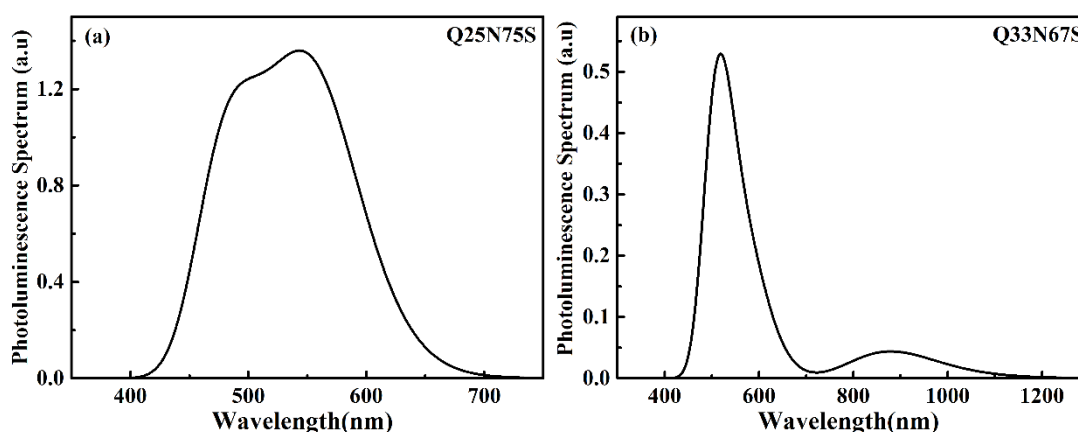


Figure S9 The combination of the emission of selected configurations of Q25N75S and Q33N67S glasses. Assuming the photoluminescence originates from the lowest-energy transition with the same oscillator strength, the PL spectrum was obtained by combining the photoluminescence of each configuration. The oscillator strength and excitation energy were broadened by the Gaussian function with a line width of 150 meV to obtain the photoluminescence spectra.